Lasers in Surgery and Medicine 45:450–459 (2013)

Safety Evaluation of Femtosecond Lentotomy on the Porcine Lens by Optical Measurement with 50-Femtosecond Laser Pulses

Jiaying Zhang, MD,[1,2†] Rui Wang, MS,[2†] Bing Chen, MS,[3] Peng Ye, MS,[2] Wei Zhang, MS,[2] Hongyou Zhao, MS,[1] Jie Zhen, MS,[4] Yifei Huang, MD,[3] Zhiyi Wei, PhD,[2*] and Ying Gu, MD[1*]

[1]*Department of Laser Medicine, General Hospital of PLA, Beijing, 100853, China*

[2]*Beijing National Laboratory for Condensed Matter Physics and Institute of Physics, Chinese Academy of Sciences, Beijing, 100190, China*

[3]*Department of Ophthalmology, General Hospital of PLA, Beijing, 100853, China*

[4]*School of Information and Electronics, Beijing Institute of Technology, Beijing, 100081, China*

Background and Objective: The optimized parameters of femtosecond (fs) lentotomy, an innovative strategy for presbyopia, have been further discussed regarding the safety of the procedure for eyeballs. This article's aim was to prove the safety and feasibility of the fs lentotomy procedure with 50-fs laser pulses.

Study Design/Materials and Methods: This was an experimental study in which the safety of fs lentotomy by optical measurement was tested. The experiment was performed on 49 porcine crystalline lenses by 50-fs laser pulses at a central wavelength of 800 nm and scanning focusing optics with a numerical aperture (NA) of 0.125. The input pulse energy was in the range of 0.35 μJ to 0.65 μJ. The transmitted energy throughout the eyeball was measured through a hole in the back wall of the eyeball by a power meter. The transmittance and peak power density (PPD) on the cornea, lens, and retina were illustrated. The laser cutting quality of 50-fs laser pulses on the crystalline lens were assessed, and the theoretical safety of such a procedure for the cornea, lens, and retina was evaluated.

Results: A sharp cut without noticeable large bubbles was obtained with 0.35 μJ pulse energy under the optical system for which the NA was 0.125. The transmittance of the whole eyeball was measured to be 69% to 75% under 0.35 μJ to 0.65 μJ incident laser energy. The threshold of PPD for photodisruption on the crystalline lens, retina, and cornea was measured to be in the magnitude of 10^{13} W/cm^2, 10^8 W/cm^2, and 10^9 W/cm^2, respectively.

Conclusions: The cutting quality in this experiment implied the feasibility of the 50-fs laser in fs lentotomy; the pulse energy for fs lentotomy descended from microjoules to hundreds of nanojoules, and the PPD on the cornea and retina during the procedure decreased further, both of which illustrated the safety of such an optical design and the parameters during fs lentotomy for the eyeball. Lasers Surg. Med. 45:450–459, 2013.

Key words: accommodation; crystalline lens; laser surgery; photodisruption; presbyopia

INTRODUCTION

In the past decade, the femtosecond (fs) laser-induced crystalline lens-cutting procedure (i.e., fs lentotomy) was suggested by Lubatschowski et al. [1–13] as an effective and safe strategy and a potential dynamic accommodating method to relieve presbyopia. In 2008, Ripken et al. investigated the change of lens deformability due to different numbers, positions, and alignments of gliding planes produced by the laser inside the lens, and found the deformation ability of enucleated porcine lenses increased up to 26% after the laser intervention [1]. In 2009, Schumacher et al. showed an increase of 16% in deformation ability of the human donor lens after fs lentotomy at a rotational speed of 1,620 rpm during the Fisher spinning test [11]. The results of 14 cases of presbyopia operated on using fs lentotomy in the Philippines in 2009 did not show that the postoperative accommodation of a crystalline lens enhanced significantly, which implied that the effect of this innovative surgical method on presbyopia had to be further improved. Redesigning the cutting pattern inside the crystalline lens according to the lens' biomechanical characteristics is one of the ways to improve the unsatisfactory surgical results. An available method to evaluate the

Conflict of Interest Disclosures: All authors have completed and submitted the ICMJE Form for Disclosure of Potential Conflicts of Interest and none were reported.

The funding organizations had no role in the design or conduct of this research.

†The first two authors contributed equally to the current work.

Contract grant sponsor: National Important Scientific Instruments and Equipments Developing; Grant number: 2012YQ 03012607

*Correspondence to: Ying Gu, Department of Laser Medicine, General Hospital of PLA, No. 28, Fuxing Road, Beijing, China 100853. E-mail: guyinglaser@sina.com
and Zhiyi Wei, PhD, Beijing National Laboratory for Condensed Matter Physics and Institute of Physics, Chinese Academy of Sciences (CAS), No. 8, South 3rd Street, Zhongguancun, Beijing, China 100190. E-mail: zywei@iphy.ac.cn

Accepted 10 May 2013
Published online 7 August 2013 in Wiley Online Library (wileyonlinelibrary.com).
DOI 10.1002/lsm.22154

© 2013 Wiley Periodicals, Inc.

crystalline lens' elasticity *in vivo* is necessary to develop the remedy for presbyopia in the lab as well as in the clinic.

On the other hand, postoperative crystalline lens collagen fibroblasts found in previous research, as well as in our trials, appeared to be burnt at the laser cutting sites as long as 6 months after surgery, although the cataract was always absent [12,13]. The remaining cutting pattern, when residual bubbles moved to the optical axis, induced dazzle and a halo effect to the postoperative eye, which negatively affected the patients' vision. Because of that, a dissatisfied postoperative accommodation was reported by Krueger et al. at the annual meeting of the American Society of Cataract and Refractive Surgery in 2011. Meanwhile, conclusions with respect to fs lentotomy safety were drawn from structural observation through slit lamp and pathological examination after surgery [6,12,13], instead of the functional evaluation of relative tissues where functional change always arises ahead of histostructural change. All of the above prompted the necessity to carefully optimize the parameters of an innovative strategy for presbyopia to improve its actual effect and safety.

Laser energy is strongly correlated with tissue damage. The same effect of laser-induced optical breakdown (LIOB) in this cutting procedure can be realized with pulse energy lower than microjoule magnitude through compressing pulse width further to be $<$100 fs. In this study, we simulated the surgical process using a 50-fs titanium (Ti): sapphire laser at a repetition rate of 1 kHz, with an optical lens at a 40-mm focal length, to test the safety of fs lentotomy by optical measurement. The transmittance of the whole eyeball was measured to be 69% to 75% under the incident pulse energy of 0.35 μJ to 0.65 μJ. When a sharply cut profile without obvious large bubbles appeared, the peak power densities (PPDs) on the crystalline lens, retina, and cornea were in the magnitude of 10^{13} W/cm^2, 10^8 W/cm^2, and 10^9 W/cm^2, respectively. Referring to the previous reports on the damage threshold of fs laser to eye, the theoretical feasibility and safety of the innovative procedure were verified [14–21]. This quantitative measurement is a preliminary trial for the safety evaluation on ultrafast laser lentotomy with a shorter pulse width.

MATERIALS AND METHODS

Experimental Model and Setup

The light path inside the eyeball was simulated according to the Gullstrand optical eye model (Table 1), which provided a referred distance of 32 mm from the exit pupil of the F-theta lenses to the corneal surface of the porcine eyeball along the primary optical axis. Given the incomplete back wall of the eyeball designed for measuring and the flattened cornea in the experiment (the partial removal of the eyeball's back wall made the intraocular pressure lower than normal, and thus the cornea was flattened further), the laser beam was adjusted to focus ~3.5 mm behind the corneal surface, which was estimated at ~1.5 mm beneath the anterior capsule of the crystalline lens (Fig. 1).

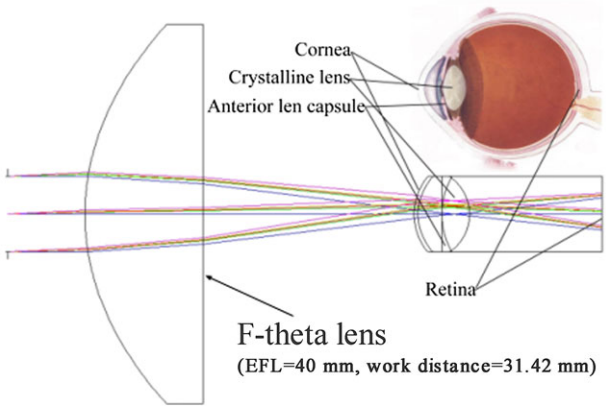

Fig. 1. Schematic diagram of the simulated optical path of the laser in the eye. EFL, effective focus length.

The experimental setup is shown schematically in Figure 2. The fs Ti:sapphire amplifier (made by the Chinese Academy of Sciences, Institute of Physics) had a maximum output pulse energy of 1.5 mJ with a pulse duration of 35 fs at the central wavelength of 800 nm and the repetition rate of 1 kHz. The diameter of the output beam was 10 mm after collimation. The laser beam was scanned by a two-dimensional scanning galvanometer in the x-y plane and a linear translation stage along the z-axis inside the crystalline lens. A set of custom-made achromatic F-theta lenses (Lenstec, Wuhan, China), with a focal length of 40 mm and a corresponding numerical aperture (NA) of 0.125, focused the laser beam to a spot with a minimum diameter of 8 μm (1/e^2, the diameter size of the focal spot when its light intensity decreased to 1/e^2 of the maximum). The center part of the focus pattern presented a Gaussian distribution recorded by a charge-coupled

TABLE 1. Parameters of Gullstrand eye model

Eyeball	Parameters	Refraction radius (mm)	Refraction indice		Refraction power (D)
Cornea	anterior surface	7.8		1.376	43.05
	posterior surface	6.8			
Crystalline lens	anterior surface	10.0	Cortex	1.386	19.11
	posterior surface	6.0	Core	1.406	
Aqueous & vitreum				1.336	
Whole eyeball					58.64

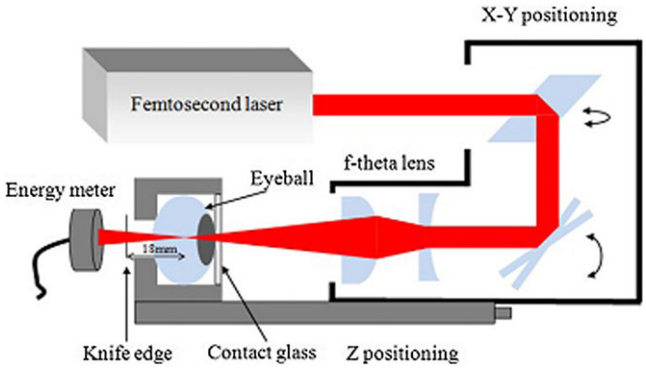

Fig. 2. Schematic layout of the cutting and testing setup.

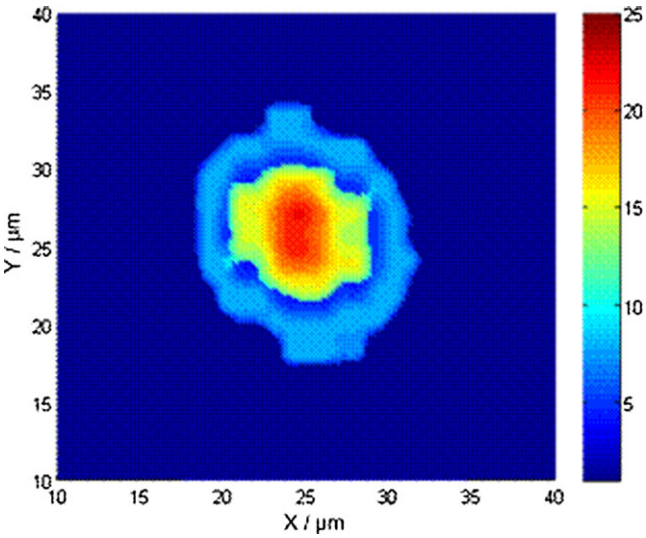

Fig. 3. Intensity distribution of the focus spot.

device (CCD) (WAT-902B; Watec, Yamagata, Japan) in the air (Fig. 3). Taking the group velocity dispersion introduced by the air, optics, and intraocular components into consideration, positive dispersion was precompensated in the compressor to ensure the shortest pulse duration in the crystalline lens. Then the three main aberrations—chromatism, spherical aberration, and dispersion—in our experiment were reduced by achromatic optics, relatively low NA, and negative pre-chirp. The pulse width in front of the eyeball was measured to be about 50 fs after being stretched by the lenses throughout the optical path.

Eyes

Forty-nine fresh eyeballs of 8- to 12-month-old pigs were obtained from a nearby abattoir within 2 hours after slaughter and kept on ice within 2 to 6 hours after enucleation before usage to preserve the transparency of the cornea and lens. The eyeballs were randomly divided into seven groups according to different incident pulse energies. In each group, four crystalline lenses were cut *in situ*, and the other three were cut after being extracted from the eyeballs. For the cut *in situ*, the eyeball was mounted onto a customized holder with a coverslip flattening the surface of the cornea to reduce the scatter introduced by the curvature. Similarly, the extracted crystalline lens was placed in a special groove and covered with a piece of coverslip to flatten its front surface during the cut.

Cutting Pattern

The steering-wheel cutting pattern recommended by Lubatschowski et al. [12] was adopted. It was designed with an inner radius of 0.5 mm, outer radius of 2 mm, depth of 1.5 mm, and 12 radial sections (Fig. 4). The separations of adjacent laser spots were 10 μm in the x-y plane and 50 μm along the z-axis. The cutting profiles were observed through a 6.3× to 50× zoom stereo microscope (XSZ-107E; Ningbo Biocotek Scientific, Ningbo, China).

Transmittance and Spot Size Determination

With respect to the threshold of fs laser-induced optical breakdown to biological tissues shown in previous research [1,6,22], the incident laser energy in our experiment was set within a range of 0.35 μJ to 0.65 μJ. The transmitted energy of the beam through the whole eyeball (cornea, aqueous humor, lens, and vitreous) was recorded by a power meter placed after the vitreous when the central retina and sclera were partially removed [23]. The hole on the back wall of the eyeball was ~7 mm in diameter so as to permit the whole transmitted beam to enter into the probe of the power meter, even during the scanning process. The transmitted energy oscillated at different incident angles due to the surface curvature of the lens and the different optical paths when scanning. The maximum transmittance value was employed to estimate the safety to the retina. To calculate the PPDs on the cornea, crystalline lens, and retina, the sizes of the beam spots falling on the cornea and retina were simulated by Zemax optical simulation software (Radiant Zemax, LLC, Redmond, WA) and measured by the knife-edge method, in addition to the size of the focus spot.

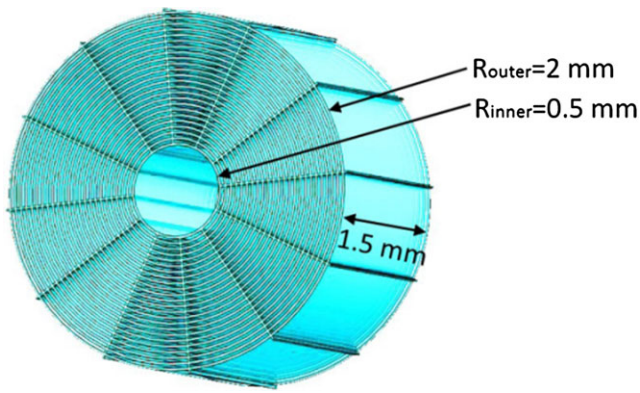

Fig. 4. Schematic diagram of the steering wheel cutting pattern. R_{inner}, inner radius; R_{outer}, outer radius.

RESULTS

Cutting Results

The cutting quality was characterized by the size and number of bubbles that were produced by cavitation during LIOB according to previous research [1,4,13]. Bubble amount was quantitatively analyzed by ImageJ software (National Institutes of Health, Bethesda, MD). The ratio of bubble-covered area in a selected region on one section among the cutting patterns under different incident pulse energies (0.32 μJ–0.8 μJ) was calculated by ImageJ, which is diagrammed in Figure 5. The bubble size and the sharpness of the cutting edge were reasonably estimated by a scale bar provided in Figure 6. Minimal amounts of microbubbles allowed for sharp cutting curves. For cutting *in situ*, the threshold pulse energy was 0.35 μJ (Fig. 6A) with the PPD at $\sim 10^{13}$ W/cm^2 for photodisruption. When increasing the input pulse energy to 0.4 μJ, sharp cutting patterns without noticeable large bubbles appeared (Fig. 6B). For cutting inside extracted lenses, the input energy of 0.35 μJ made satisfactory profiles (Fig. 6D). In contrast, when the pulse energy was increased to 0.5 μJ, numerous unwanted large bubbles emerged during cutting whether *in situ* (Fig. 6C and Fig. 7) or after extraction (Fig. 6F). The size and number of large bubbles increased with enhanced input energy. On the other hand, cutting *in situ* resulted in fewer and smaller bubbles than those inside the extracted lenses, even under the same incident pulse energy. Also, cutting in the frontal area made fewer and smaller bubbles than in the sagittal star-like section. A majority of bubbles disappeared in a few minutes, with large bubbles disappearing more slowly than small ones.

Distribution of Light

The pulse energy of the incident beam was reduced after passing through the eyeball. On average, 30% of the input energy was consumed throughout the eye (Fig. 8, black linear fitting line). The PPD on the cornea was estimated at $\sim 10^9$ W/cm^2 given the measured beam size of 764 μm in diameter (Fig. 9). The PPD on the retina was $\sim 10^8$ W/cm^2 when the transmitted light spot irradiating it was measured at 2.96 mm in diameter and the input energy was <0.65 μJ (Fig. 8, red linear fitting line; Fig. 9).

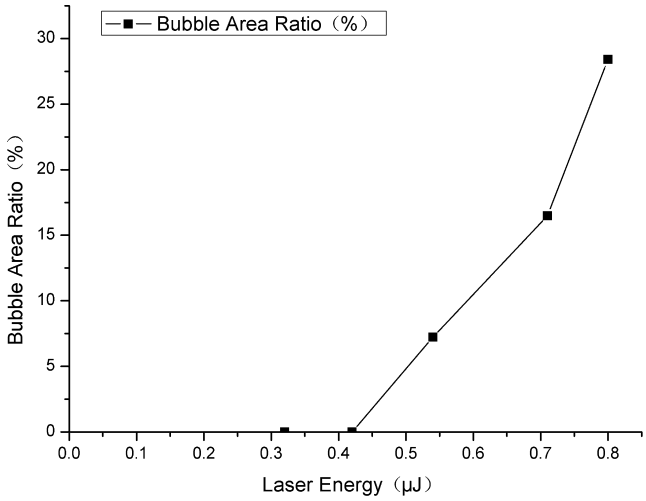

Fig. 5. The ratio of the bubble-covered area in a selected region in one section among the cutting patterns under different incident pulse energies (0.32 μJ – 0.8 μJ), calculated by ImageJ software.

DISCUSSION

Cornea and Retina Safety

The transmittance during the fs lentotomy procedure was defined as the percentage of the pulse energy passing through the eyeball versus the input pulse energy. We found that when the incident energy was in the range of 0.35 to 0.65 μJ, the average value of the transmittance was 69.8% and increased to 75% (Fig. 8, black line). It appeared that, although the nonlinear effect, such as two-photon absorption or multiphoton absorption, strengthened along with the increase of input energy, the energy consumed during this cutting procedure tended to saturation when the input energy increased to a certain level. The redundant energy transmitting toward retina could induce intraocular damage. That was one of the reasons for exploring the optimal parameters during laser-assisted surgery.

Owing to the regular arrangement of collagen fibers and high water content, cornea and crystalline lenses are regarded as almost wholly transparent to near infrared (NIR) light (as are the aqueous humor and vitreous body). The decrease of incident energy after passing through the eyeball in this investigation may have arisen from three factors: (i) the transformation of light energy to nonlinear absorption during the lens cutting procedure; (ii) inelastic light scattering by the front surface of lens (instead of the front surface of cornea, which was flattened by a coverslip in the experiment); and (iii) light scattering caused by gas bubbles generated during cavitation. Analyzing the structure of our system and experiment results, we concluded that the contribution of inelastic scattering can be neglected (see the detailed analysis in Appendix 1.). On the contrary, light scattered by gas bubbles should be paid more attention and discussed thoroughly. For the transmittance evaluation experiment, the laser was only scanned in the x-y plane instead of along the z-axis. Therefore, the light scattering caused by the bubbles on previous cutting planes was avoided. Taking the spot separation in the same plane into consideration, the bubbles generated by the former pulse, whose sizes were >10 μm, did have the opportunity to scatter the latter pulse. In our experiment, the biggest bubble caused by 0.65 μJ input power was estimated to be ~40 μm in diameter after 1-ms (pulse interval of the laser) evolution. Therefore, the light scattered by 10 μm to 40 μm gas bubbles should be investigated. The light was mainly scattered in the angle range of 0.49° to 1.98° suggested by the Mie scattering model shown in Equation (1) and Figure 10. The corresponding maximum scattering radius was 5.8 mm, in view of the focusing optical path, the outer

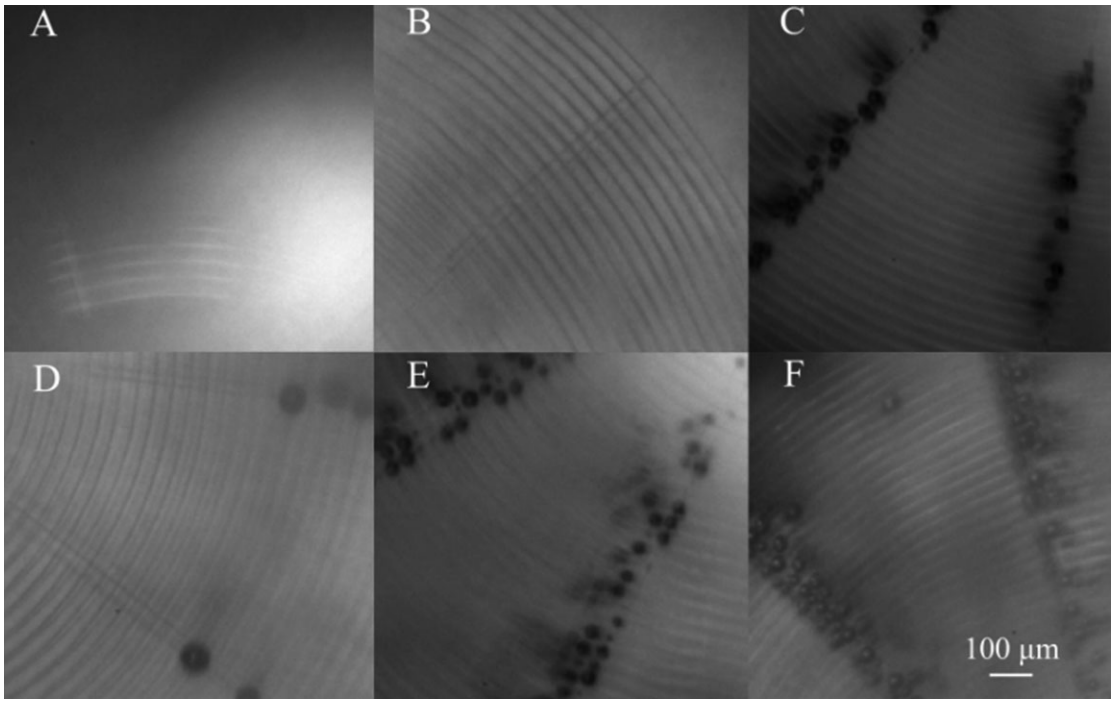

Fig. 6. Variations of the cutting effect characterized by the size and amount of bubbles and the sharpness of the cutting edge with incident pulse energy. The larger the pulse energy applied, the more and bigger the bubbles that were generated, and the rougher the cutting edge. **(A–C)** In situ cutting. **(D–F)** Cutting inside extracted lenses. For each group, three pulse energies, 0.35, 0.4, and 0.5 μJ, were applied. The different brightness levels of the bubbles in the photos resulted from different illuminations when taking the photos.

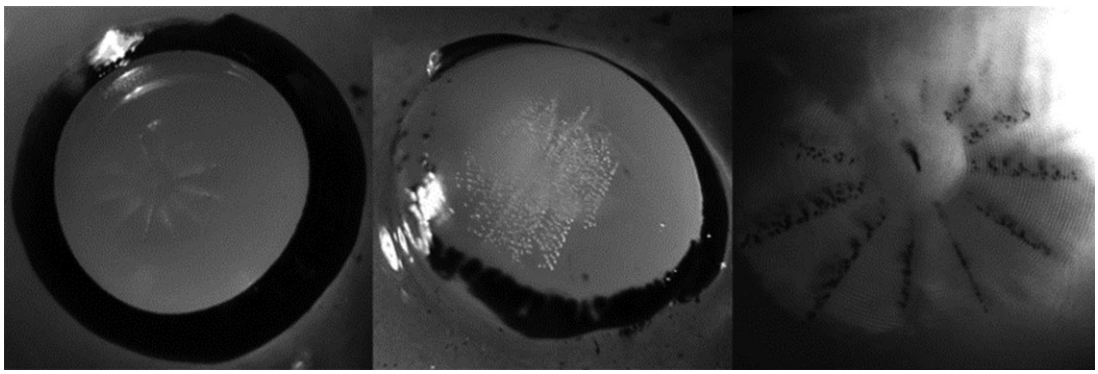

Fig. 7. The integral cutting results of one crystalline lens shows the even distribution of cutting with 0.5-μJ pulse energy. All photos were taken with a camera from different angles using different magnifications.

radius of the cutting pattern (2 mm), and the distance between the cutting position and the power meter (18 mm). As a result, the transmitted energy we measured had already included the forward scattering light caused by bubbles given the radius of the detector's active area of 7.5 mm. Meanwhile, the backward scattering could be ignored, because it plays an important role in scattering short wavelength light, such as blue light, instead of NIR light. Consequently, the reduction of the input energy we measured in this investigation was mainly accounted for by nonlinear absorption. As shown in Figure 7, 25% to 30.6% of the incident energy was consumed in the LIOB, which was right in the range of the theoretical absorption rate (16%–30%) of fs photodisruption (including two main mechanical processes: acoustic shock wave [1%–5%] and cavitation [15%–25%]) [24–26].

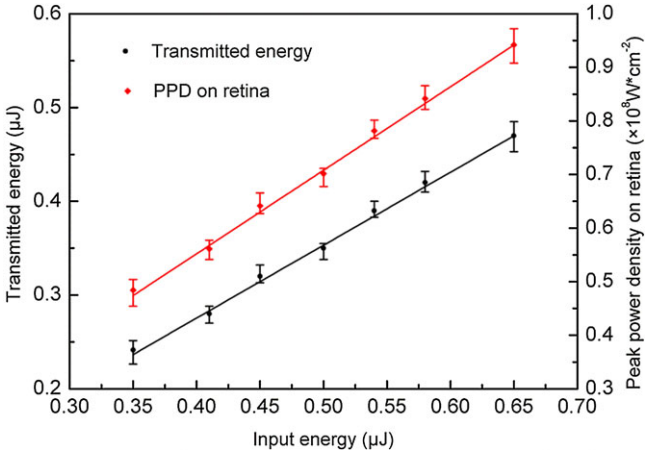

Fig. 8. Laser energy transmitted through the eyeball. The graph shows the mean (±standard deviation, n = 4) transmitted energy and peak power density (PPD) versus input energy. The linear fitting lines were described by the functions of y = 0.77776x − 0.03567 (for transmitted energy, black line) and y = 1.55895x − 0.07151 (for PPD, red line).

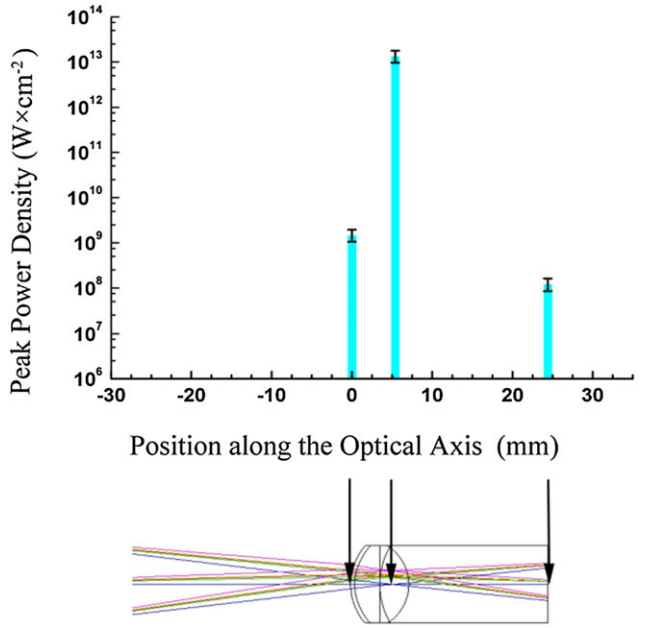

Fig. 9. Peak power density on the cornea, crystalline lens, and retina.

$$\tan\theta = 1.357\lambda/\pi d \quad (1)$$

In Equation (1), θ is max scattering angle, λ is wavelength of laser, and d is diameter of the bubble.

The safety of the procedure for the cornea and retina was evaluated by PPD. The measured diameter (764 μm) of the beam on the cornea agreed with the simulated value (774 μm) of Gullstrand model eye. The calculated PPD of 1.53×10^9 to 2.84×10^9 W/cm^2 on the cornea was much lower than the fs photodisruption threshold of 2×10^{13} W/cm^2 [27], thus the cornea was theoretically safe during the procedure. On the other hand, the measured diameter

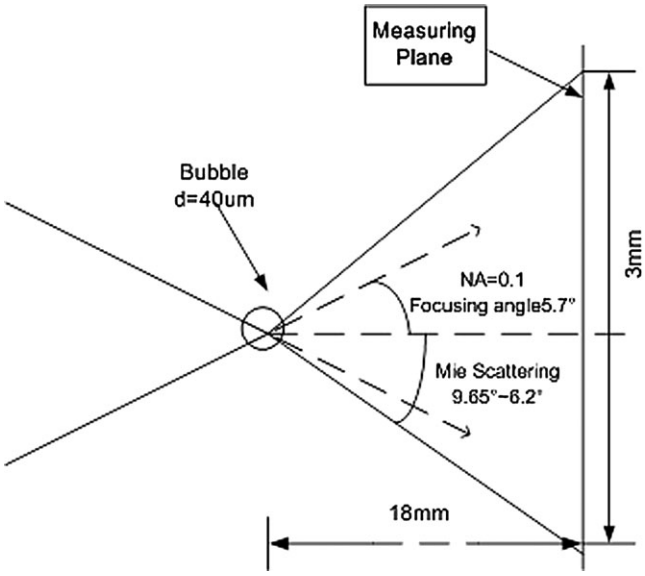

Fig. 10. Mie scattering model.

(2.96 mm) of the beam on the retina was slightly larger than the simulated value (2.84 mm). The discrepancy arose probably from the size variability between human and porcine eyeballs. Also, the porcine cornea was flattened, and a hole was made at the back wall of the eyeball in this study, both of which changed the axial length of the eyeball. Fortunately, the inconsistency had no effect on the calculated PPD on the retina, which was in the range of 7.10×10^7 W/cm^2 to 1.42×10^8 W/cm^2. Referring to the International Electrotechnical Commission guidelines for the safe use of lasers (IEC 60825-1, 2007) [28], the maximum permissible exposure on cornea for multiple pulses with a wavelength of 800 nm and pulse duration of 100 fs or less is ~10 nJ/cm^2 (~10^5 W/cm^2) [24]. Due to the refraction of the cornea and crystalline lens, the intensity of incident light is enhanced $10^5\times$ when it arrives at the retina (US Occupational Safety & Health Administration Technical Manual) [29]. The light intensity that the retina can stand should be about 10^{10} W/cm^2. The deduction process is shown in Appendix 2. Our measured result was far from this criterion, especially considering that the laser pulse should be stretched considerably when arriving at retina. The irradiation exposure at the retina was theoretically safe during the procedure. In addition, the macular zone was safe, as only ~30% of NIR light energy can be absorbed in that area [25].

We simulated the temperature rise of the retina during laser surgery from the energy absorption by retinal pigment epithelium according to Sun's model [30,31]. The maximum temperature rise was simulated to be 0.024°C, with 0.65 μJ input energy at a 1-kHz repetition rate under our optical system and 2.353°C at 100 kHz (Fig. 11). In providing the threshold for thermal damage on the retina (~40°C), the fs lentotomy procedure with the present laser parameters delivered no thermal hazard to the retina through temperature increase.

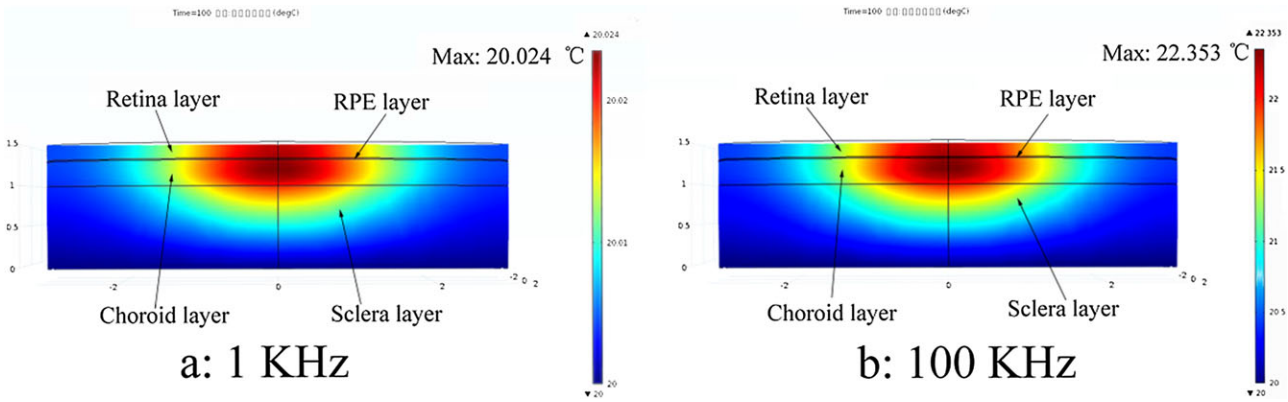

Fig. 11. Simulation of the temperature distribution in the retina under 0.65 μJ input energy at a repetition rate of 1 kHz (left) or 100 kHz (right) during the 100-second period of the fs lentotomy procedure. Assume that the surrounding temperature of 20°C is a boundary condition. RPE, retinal pigment epithelium.

When propagating through uniform medium, the Gaussian beam will maintain its Gaussian spatial distribution of intensity. If the strongest central part creates no damage to eye tissue, we can say the eye is unharmed by the laser. However, if the medium is nonuniform or there are some large particles, the Gaussian beam will change its intensity distribution when passing through the medium. Due to diffraction, scattering, and nonlinear effects, there may be some hot spots in the beam, the intensity of which may be strong enough to harm eye tissue. Another potential hazard may be caused by distortions of irradiance distribution on the retina; therefore, the beam profile propagating through the whole eyeball is recorded by a CCD. Although the interaction between adjacent bubbles existed, the main part of the distribution was distinguished. No "hot point" appeared in the beam distribution on the retina (Fig. 12); therefore, the retina was considered to be safe. The calculated PPD on the retina (Fig. 8, red line; Fig. 9) was further proven to be valid in evaluating the safety of this strategy.

Safety and Efficacy for the Crystalline Lens

The safety of the procedure with respect to the crystalline lens itself was also analyzed. For fs laser, the threshold of PPD for LIOB is around 10^{12} W/cm^2. Under the same PPD, the larger the pulse energy the stronger the thermal effect, and therefore more serious accessory injury to tissue is induced. Photodisruption inside the lens led to a shock wave and cavitation bubbles, both of which produced side effects on the tissue surrounding the focus and then ruined the high accuracy of fs laser surgery. Our study showed the relevance of occurrence and increase of bubbles to the pulse energy (Fig. 5, Fig. 6, and Fig. 7), which was consistent with previous research [32]. Sharp cutting profiles without noticeable large bubbles were achieved by a pulse energy of 0.4 μJ for cutting *in situ* and 0.35 μJ for cutting extracted lenses in our experiment, in contrast to ~1 μJ in previous work [1,32], through compressing the pulse duration further from hundreds of fs to tens of fs. Theoretically, the accessory injury to eye tissue, including the crystalline lens, caused by the laser in our experiment should be reduced due to the weakened pulse energy, although detailed information has to be presented in the future. The different cutting effects between the cutting *in situ* and on dissected lenses with the same pulse energy perhaps result from the refraction of the front surface of the crystalline lens and the distortion of nonlinear

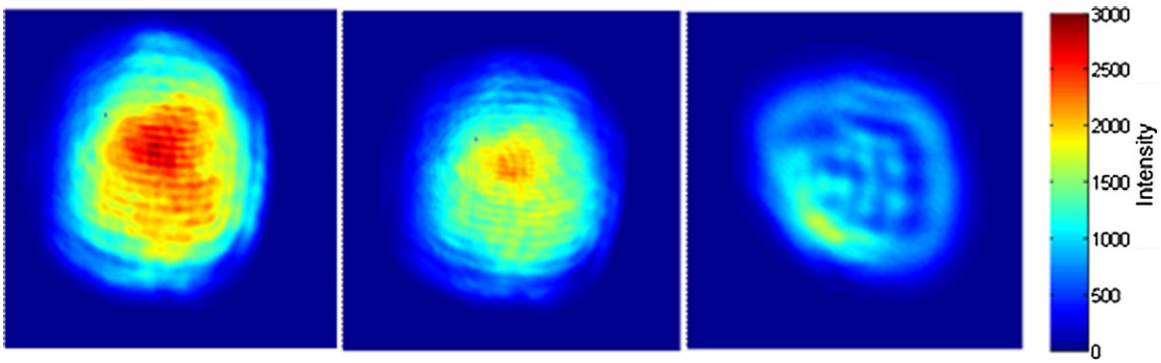

Fig. 12. Intensity distribution of a light spot recorded by a charge-coupled device at the retina level. The three samples are from different porcine eyeballs. The color represents the intensity of light on the retina.

propagation in the eyeballs, which was more serious than that in the air.

The threshold of photodisruption in the crystalline lens in our experiment was 1.39×10^{13} W/cm^2, which is in agreement with previous research [31] and a bit higher than the theoretical value of 3×10^{12} W/cm^2 for a 100-fs pulse in water. On the other hand, our calculated PPD value was a bit higher than the threshold of self-focusing, and as a result the existence of supercontinuum and filamentation had to be discussed. The emergence of supercontinuum or filamentation is related not only to self-focusing but also to the NA value of the optical system. Liu et al. [33] studied the threshold of filamentation and optical breakdown in water as a function of NA; the threshold of optical breakdown was lower than that of filamentation (3.4×10^{14} W/cm^2) when NA was 0.125, even under the pulse energy of 0.65 μJ. Given ~65% of water content in the crystalline lens [34], no filamentation or supercontinuum was expected to occur in our experiment, and none was observed.

The application of microjoule fs laser pulses in ophthalmology has been demonstrated to be effective and safe. Nevertheless, because reversible visual problems such as light sensitivity and macular hemorrhage may occur after fs–laser-assisted stromal *in situ* keratomileusis (LASIK) in the clinic [35], more studies on optimized parameters for the safe application of the fs intraocular scheme have to be carried out. In general, photodisruptive collateral effects are correlated to pulse energy, pulse duration, and geometrical focus structure.

There are theoretically two ways to lower pulse energy further while maintaining photodisruption. One way is to apply the F-theta lens of a high NA value in the system to make focusing more compact; however, the design of such an apparatus is not easy and still a great challenge for fs laser owing to optical aberrations. Tight focusing means that the focus length of the lens is short. In this condition, two main problems will be encountered and make designing and producing the optical system hard. First, optical equipment would have to be closer to the eye. However, considering eye structure and surgical operability, the distance between the optical system and crystalline lens is limited. Second, the shorter the focal length is the more severe the aberration will be. Especially for the fs laser, a large spectrum range makes the chromatic aberration intractable.

The other way to lower pulse energy further while maintaining photodisruption is to compress pulse duration more tightly, which has been well solved in many laser groups [36,37]. The next mission is to recognize the stability and feasibility to apply ultrashort laser pulses in the clinic. In this study, we dropped pulse energy to 350 nJ during the fs lentotomy procedure by compressing pulse duration to 50 fs and verified the possibility of accomplishing such a system and its theoretical safety. Trials to lower the pulse energy in laser medical applications are promising.

ACKNOWLEDGMENTS

The authors acknowledge support from Beijing National Laboratory for Condensed Matter Physics and Institute of Physics, Chinese Academy of Sciences, where the experiments were performed.

APPENDIX 1

Inelastic scattering of light usually involves the third order nonlinear optical effect, in which the wavelength change is so little that this minor change cannot be measured. Analyzing the structure of our system and experiment results, we conclude that the contribution of inelastic scattering can be neglected.

Change of Refractive Index

The crystalline lens is mainly made up of water; therefore, we discuss the linear and nonlinear effects of water instead of the crystalline lens.

Generally speaking, a change of the refractive index would induce the scattering of light.

First, we analyze elastic scattering by bubbles. The size of the bubbles is 10 μm to 40 μm in the crystalline lens. The diameter of the focus spot is about 10 μm. The two sizes are similar; therefore, the bubbles will dramatically change the index in the focus region. The refractive index of air is about 1, and that of water is about 1.33, so δn is at the level of 0.1.

Second, we estimate δn induced by the third order nonlinear effect. We can calculate the refractive index using Equation (A1). The intensity at focus is about 10^{13} W/cm^2, the n_2 of water is 4.1×10^{-16}cm^2/W; therefore, the change of n is about 10^{-3}. The intensity-dependent refractive index is n_2.

$$n = n_0 + n_2 I \tag{A1}$$

Comparing the two conditions above, the refractive index change due to bubbles is two orders larger than that due to the third order nonlinear optical effect. Therefore, we believe that elastic scattering by bubbles dominates.

Experiment Results

Usually for the strong self-focusing and supercontinuum, inelastic scattering will take place simultaneously, as with the Raman effect. In our experiment, no obvious supercontinuum occurred; therefore, we think inelastic scattering was weak.

All nonlinear optical parameters come from Boyd and Fischer [38].

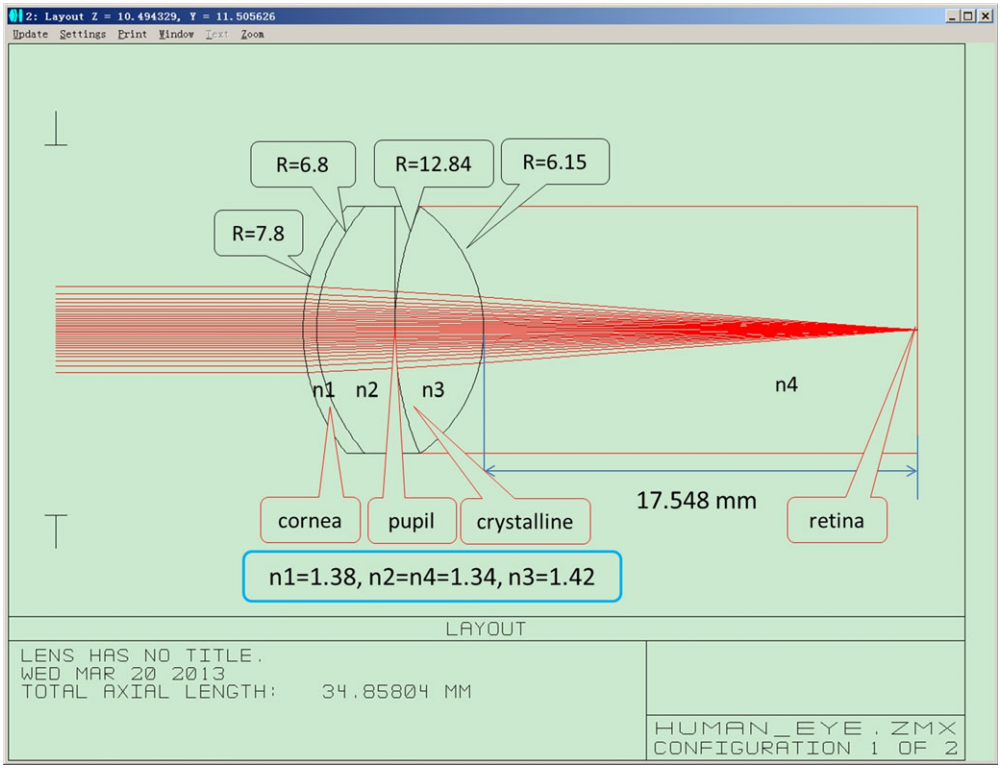

Fig. A1. Simulation of light propagating through eye.

APPENDIX 2

We use Zemax software to simulate the effect of the laser beam on the eye (Fig. A1). Assuming 1 W on a beam with a diameter of 3.5 mm, there will form an intensity of about

$$\frac{\text{power}}{\pi * r^2} = \frac{1W}{\pi \times (1.75e-1)^2} = 10.4\text{W/cm}^2 \tag{A2}$$

on the cornea. However, due to the focusing of the eye, the spot on the retina can be as small as 10.6 μm in diameter. If the incident power of 1 W does not decrease, the intensity would be

$$\frac{\text{power}}{\pi * r^2} = \frac{1W}{\pi \times (5.3e-4)^2} = 1137467\text{W/cm}^2. \tag{A3}$$

Therefore, from the estimation, the intensity on the retina will increase about 10^5 compared with that on the cornea.

REFERENCES

1. Ripken T, Oberheide U, Fromm M, Schumacher S, Gerten G, Lubatschowski H. Fs-laser induced elasticity changes to improve presbyopic lens accommodation. Graefes Arch Clin Exp Ophthalmol 2008;246:897–906.
2. Heisterkamp A, Ripken T, Oberheide U, Kermani O, Mamom T, Drommer W, Ertmer W, Lubatschowski H. Applications of ultrafast lasers in ophthalmology. Proc SPIE 2003;5142:146–153.
3. Heisterkamp A, Mammon T, Kermani O, Drommer W, Welling H, Ertmer W, Lubatschowski H. Intrastromal refractive surgery with ultrashort laser pulses: In vivo study on the rabbit eye. Graefes Arch Clin Exp Ophthalmol 2003;241:511–517.
4. Ripken T, Heisterkamp A, Oberheide U, Krueger RR, Luetkefels E, Drommer W, Ertmer W, Lubatschowski H. First in vivo studies of presbyopia treatment with ultrashort laser pulses. Proc SPIE 2003;5142:137–145.
5. Ripken T, Oberheide U, Ziltz C, Ertmer W, Gerten G, Lubatschowski H. Fs-laser induced elasticity changes to improve presbyopic lens accommodation. Proc SPIE 2005;5688:278–287.
6. Krueger RR, Kuszak J, Lubatschowski H, Myers RI, Ripken T, Heisterkamp A. First safety study of femtosecond laser photodisruption in animal lenses: tissue morphology and cataractogenesis. J Cataract Refract Surg 2005;31:2386–2394.
7. Stachs O, Schumacher S, Hovakimyan M, Fromm M, Heisterkamp A, Lubatschowski H, Guthoff R. Visualization of femtosecond laser pulse-induced microincisions inside crystalline lens tissue. J Cataract Refract Surg 2009;35:1979–1983.
8. Schumacher S, Fromm M, Lakharia R, Schaefer M, Oberheide U, Ripken T, Breitenfeld P, Gerten G, Ertmer W, Lubatschowksi H. Fs-laser induced flexibility increase in the crystalline lens. Proc SPIE 2007;6426:35–44.
9. Schumacher S, Oberheide U, Theuer H, Fromm M, Ripken T, Gerten G, Ertmer W, Lubatschowski H. fs-lentotomie: changing the accommodation amplitude of presbyopic human lenses by fs laser pulses. Proc SPIE-OSA Biomed Optics 2007;6632:66321G1–66321G10.
10. Gerten G, Ripken T, Breitenfeld P, Krueger RR, Kermani O, Lubatschowski H, Oberheide U. In vitro and in vivo investigations on the treatment of presbyopia using femtosecond lasers. Ophthalmologe 2007;104:40–46.
11. Schumacher S, Oberheide U, Fromma M, Ripken T, Ertmer W, Gerten G, Wegener A, Lubatschowski H. Femtosecond laser induced flexibility change of human donor lenses. Vision Res 2009;49:1853–1859.
12. Lubatschowski H, Schumacher S, Fromm M, Wegener A, Hoffmann H, Oberheide U, Gerten G. Femtosecond lentotomy: generating gliding planes inside the crystalline lens to regain accommodation ability. J Biophoton 2010;3:265–268.
13. Schumacher S, Oberheide U, Fromm M, Ertmer W, Gerten G, Wegener A, Lubatschowski H. Fs-lentotomy: first in vivo studies on rabbit eyes with a 100 kHz laser system. Proc SPIE 2008;6844:68440V.
14. Juhasz T, Loesel FH, Kurtz RM, Horvath C, Bille JF, Mourou G. Corneal refractive surgery with femtosecond laser. IEEE J Quantum Electron 1999;5:902–909.
15. Liu X, Kurtz R, Braun A, Liu H, Sachs Z, Juhasz T. Intrastromal corneal surgery with femtosecond laser pulses. Conf Lasers Electro Optics 1997;11:169.
16. Vogel A, Noack J, Nahen K, Theisen1 D, Busch S, Parlitz U, Hammer DX, Noojin GD, Rockwell BA, Birngruber R. Energy balance of optical breakdown in water at nanosecond to femtosecond time scales. Appl Phys B 1999;68:271–280.
17. Noack J, Vogel A. Laser-induced plasma formation in water at nanosecond to femtosecond time scales: calculation of thresholds, absorption coefficients, and energy density. IEEE J Quantum Electr 1999;35:1156–1167.
18. Cain CP, Toth CA, Noojin GD, Carothers V, Stolarski DJ, Rockwell BA. Thresholds for visible lesions in the primate eye produced by ultrashort near-infrared laser pulses. Invest Ophthalmol Vis Sci 1999;40:2343–2349.
19. Lubatschowski H. Ultrafast lasers in ophthalmology. Physics Procedia 2010;5:637–640.
20. Rockwella BA, Thomasa RJ, Vogel A. Ultrashort laser pulse retinal damage mechanisms and their impact on thresholds. Med Laser Appl 2010;25:84–92.
21. Cain CP, Dicarlo CD, Rockwell BA, Kennedy PK, Noojin GD, Stolarski DJ, Hammer DX, Toth CA, Roach WP. Retina damage and laser-induced breakdown produced by ultrashort-pulse lasers. Graefes Arch Clin Exp Ophthalmol 1996;234:28–37.
22. Lubatschowski H, Heisterkamp A. Ophthalmic applications. In: Dausinger F, Lichtner F, Lubatschowski H, eds. *Femtosecond technology for technical and medical applications*. Topics in Applied Physics 96. Heidelberg, Germany: Springer; 2004. pp 187–203.
23. Harzic RL, Buckle R, Wullner C, Donitzky C, Konig K. Laser safety aspects for refractive eye surgery with femtosecond laser pulses. Med Laser Appl 2005;20:233–238.
24. Noack J, Hammer DX, Noojin GD, Rockwell BA, Vogel A. Influence of pulse duration on mechanical effects after laser-induced breakdown in water. J Appl Physics 1998;83:7488–7495.
25. Niemz MH. Turbid media. In: Niemz MH ed. *Laser-tissue interactions: fundamentals and applications*. Heidelberg, Germany: Springer-Verlag; 2007. pp 25–27.
26. Niemz MH. Photodisruption. In: Niemz MH ed. *Laser-tissue interactions: fundamentals and applications*. Heidelberg, Germany: Springer-Verlag; 2007. pp 126–149.
27. Loesel FH, Niemz MH, Bille JF, Juhasz T. Laser-induced optical breakdown on hard and soft tissues and its dependence on the pulse duration: experiment and model. IEEE J Quantum Electron 1996;32:1717–1722.
28. Safety of laser products. Part 1: equipment classification and requirements (IEC 60825-1∗e∗d2.0). Geneva, Switzerland: International Electrotechnical Commission; 2007; pp 255–454.
29. Laser hazards. *Occupational Safety & Health Administration (OSHA) technical manual (OTM)*. Washington, DC: Occupational Safety & Health Administration; 1999.
30. Sun H, Mikula ER, Kurtz RM, Juhasz T. Temperature increase in human cadaver retina during direct illumination by femtosecond laser pulses. J Refract Surg 2010;26:272–277.
31. Sun H, Hosszufalusi N, Mikula ER, Juhasz T. Simulation of the temperature increase in human cadaver retina during direct illumination by 150-kHz femtosecond laser pulses. J Biomed Opt 2011;16:108001.
32. Ripken T, Oberheide U, Heisterkamp A, Ertmer W, Gerten G, Lubatschowski H. Investigations for the correction of presbyopia by fs-laser induced cuts. Proc SPIE 2004;5314:27–35.
33. Liu W, Kosareva O, Golubtsov IS, Iwasaki A, Becker A, Kandidov VP, Chin SL. Femtosecond laser pulse filamentation versus optical breakdown in H_2O. Appl Phys B 2003;76:215–229.
34. Fisher RF, Pettit BE. Presbyopia and the water content of the human crystalline lens. J Physiol 1973;234:443–447.
35. Principe AH, Lin DY, Small KW, Aldave AJ. Molecular hemorrhage after laser in situ keratomileusis (LASIK) with femtosecond laser flap creation. Am J Ophthalmol 2004;13:657–659.
36. Schiffrin A, Paasch-Colberg T, Karpowicz N, Apalkov V, Gerster D, Mühlbrandt S, Korbman M, Reichert J, Schultze M, Holzner S, Barth JV, Kienberger R, Ernstorfer R, Yakovlev VS, Stockman MI, Krausz F. Optical-field-induced current in dielectrics. Nature 2013;493:70–74.
37. Schultze M, Bothschafter EM, Sommer A, Holzner S, Schweinberger W, Fiess M, Hofstetter M, Kienberger R, Apalkov V, Yakovlev VS, Stockman MI, Krausz F. Controlling dielectrics with the electric field of light. Nature 2013;493:75–78.
38. Boyd RW, Fischer GL. Nonlinear optical materials. In: Buschow KHJ, Cahn RW, Flemings MC, Ilschner B, Kramer EJ, Mahajan S, Veyssiere P, eds. *Encyclopedia of materials: science and technology*. Amsterdam, the Netherlands: Elsevier Science; 2001. pp 6237–6244.